AJPR
Avicenna Journal of Pharmaceutical Research
Avicenna J Pharma Res. 2025 ;6(1):47-58
DOI: 10.53208/ajpr.6.1.47
http://ajpr.umsha.ac.ir

Original Article

Development and Toxicity Assessment of a Nano-Niosomal Preparation for Topical Delivery of Azelaic Acid

Omid Keshvari-Sharif[1], Seyed Yaser Vafaie[1], Rasool Haddadi[2], Shabnam Pourmoslemi[1]*

1. Department of Pharmaceutics, School of Pharmacy, Medicinal Plants and Natural Products Research Center, Hamadan University of Medical Sciences, Hamadan, Iran
2. Department of Pharmacology and Toxicology, School of Pharmacy, Medicinal Plants and Natural Products Research Center, Hamadan University of Medical Sciences, Hamadan, Iran

Article history:
Received: March 30, 2025
Revised: May 25, 2025
Accepted: May 27, 2025
Published: July 27, 2025

***Corresponding author:**
Shabnam Pourmoslemi, Department of Pharmaceutics, School of Pharmacy, Hamadan University of Medical Sciences, Hamadan, Iran
Tel: +989183140815
E-mail: Sh.moslem@umsha.ac.ir.

Abstract

Background: The present study aimed to design and investigate a topical preparation based on niosomal nanocarriers for local delivery of azelaic acid.

Methods: Niosomal nanocarriers were prepared using a thin-layer hydration method. Physicochemical properties of nanocarriers, including size and morphology, zeta potential, and drug entrapment efficiency, were determined. A hydrogel containing the nano-niosomes was prepared and investigated for viscosity, pH, release, and *ex vivo* skin permeability of azelaic acid. Rabbit skin irritation and cell cytotoxicity of the preparations were investigated using Draize and MTT tests, respectively.

Results: Azelaic acid containing niosomal nanocarriers were prepared in the form of homogeneous spherical vesicles, with 274.3 nm size, and +46.1 mV zeta potential. Azelaic acid entrapment efficiency was 95.1% ± 3.8%, and niosomal nanocarriers were stable at 4 and 25 °C for 3 months. The hydrogel released 89.6 ± 3.48% of azelaic acid in 24 h, and skin permeation was 77.9 ± 4.9 µg/cm^2. Toxicological investigations did not show any skin irritation or cell cytotoxicity.

Conclusion: The prepared topical preparation based on niosomal nanocarriers can be a promising approach for the local delivery of azelaic acid. It showed good physicochemical properties, sustained release, and increased skin permeation of azelaic acid, without causing any side effects.

Keywords: Azelaic acid; Hydrogel, Niosomal nanocarriers; Topical delivery

Introduction

Azelaic acid (AZA) is a natural saturated dicarboxylic acid that is found in whole grains (barley, wheat, and rye) and animal products and is used in the treatment of various skin diseases, including acne, rosacea, and hyperpigmentation [1-5]. In addition, the anti-androgenic activity of AZA is of great importance in its potential effectiveness for androgenic alopecia. AZA inhibits the activity of 5-alpha reductase, the enzyme responsible for converting testosterone to dihydrotestosterone [6]. Through reduction of the dihydrotestosterone level, AZA inhibits its damaging effect on hair follicles, especially by slowing the thinning process [7, 8]. AZA has also shown anti-inflammatory and anti-microbial effects through inhibition of leukotrienes activity and reduction of the synthesis of microbial proteins [9]. It also exerts its topical effect by normalizing the keratinization process and adjusting pigment production [10].

© 2025 The Author(s); Published by Hamadan University of Medical Sciences. This is an open-access article distributed under the terms of the Creative Commons Attribution License (http://creativecommons.org/licenses/by/4.0), which permits unrestricted use, distribution, and reproduction in any medium, provided the original work is properly cited.

[Downloaded from ajpr.umsha.ac.ir on 2026-11-05]

[DOI: 10.53208/ajpr.6.1.47]

Nano-based delivery systems have been widely considered for local delivery of drugs to the skin [11]. Nanoparticles can improve the physicochemical stability of drugs in the presence of environmental factors and increase their penetration through the skin [12]. Furthermore, sustained release of drugs increases their durability on the skin and improves the appearance of the formulation, which ultimately leads to higher patient acceptance and therapeutic efficacy of the formulation [13, 14].

Other features of nanoparticles include their high stability, biocompatibility, and specific and adjustable physical and chemical properties [15]. Niosomes are a class of vesicular nano-carriers formed by self-association of non-ionic surfactants in an aqueous phase. They are capable of carrying both hydrophilic and lipophilic drugs with high chemical stability and biodegradability, and low production cost and toxicity [16]. Niosomal delivery systems improve pharmacokinetic parameters of the drugs, thereby increasing their therapeutic effects and reducing their side effects [17].

In the present study, the thin-film hydration method was used for the preparation of niosomal nanocarriers loaded with AZA, which were then incorporated into a hydrogel preparation. Both niosomal and hydrogel preparations were fully characterized and investigated for topical delivery of AZA.

Materials and Methods

Chemicals

Azelaic acid, Span 80, cholesterol, methanol, and chloroform were purchased from Merck (Dartmouth, Germany). Carbopol 940 was obtained from Sigma (St. Louis, MO, USA). All other reagents and solvents used were purchased from Pishgaman Shimi (Tehran, Iran).

Experimental Design

A statistical optimization approach utilizing a three-level Box-Behnken (BB) scheme was employed to optimize formulation variables for the production of AZA-loaded niosomes, with high encapsulation efficiency and optimal particle size (DesignExpert® software, version 13, Stat-Ease Inc., Minneapolis, MN, USA). A total of 15 experiments (Table 1) were undertaken, with three independent variables being evaluated. The independent (high, medium, and low levels) and dependent variables are presented in Table 2. The suggested optimized formulation was then prepared and investigated (n=3) to ensure the validation of the anticipated results provided by the software.

Table 1. Formulation design for AZA niosomes

	Factor levels in actual values		
Run	**X1=AZA amount (mg)**	**X2=Total weight of niosomal ingredients (mg)**	**X3=Surfactant: Cholesterol (w/w)**
1	15	100	1
2	15	125	1.5
3	15	125	1.5
4	10	125	1
5	20	125	1
6	20	100	1.5
7	15	125	1.5
8	15	150	2
9	10	100	1.5
10	20	150	2
11	15	150	2
12	20	125	1.5
13	10	150	2
14	10	125	1.5
15	15	100	1

AZA: azelaic acid

[Downloaded from ajpr.umsha.ac.ir on 2026-11-05]

[DOI: 10.53208/ajpr.6.1.47]

Table 2. Design-Expert for optimization of the encapsulated AZA

Factors (independent variables)	Levels		
	High (+1)	Medium (0)	Low (-1)
X1: Total weight of niosomal components (mg)	150	125	100
X2: drug amount (mg)	20	15	10
X3: surfactant: cholesterol	2	1.5	1
Responses (dependent variables)		**Constraints**	
Y1: encapsulation efficiency (%)		Max	
Y2: particle size (nm)		Min	

Niosomes preparation

Thin film hydration was used to prepare niosomal nanocarriers. Certain weights of Span 80 and cholesterol, in different molar ratios (1:1, 1.5:1, and 2:1), were dissolved in 30 mL of 2:1 v/v chloroform: methanol mixture in a round-bottom flask. Subsequently, 20 mg AZA was added to the lipid mixture. A thin film was formed in the flask after the solvent was evaporated using a rotary evaporator at 35 °C.

After complete removal of the organic solvent, niosomal nanocarriers were formed by hydrating the thin film using 20 mL phosphate-buffered saline (PBS, pH 7.4) at 37 °C. To create a uniform dispersion, the resulting suspension was subjected to a 5-minute sonication process in an ultrasonic bath [18]. Blank niosomes were prepared using the same method without adding AZA to the lipid mixture.

Hydrogel preparation

Materials used for preparing the hydrogels are tabulated in Table 3. Free or encapsulated AZA was added to a glass beaker, and distilled water was gradually added while stirring. Propylene glycol, methyl paraben, and propyl paraben were added as antimicrobial preservatives, and glycerin was used to provide the hydrogel with moisture retention properties. To create a uniform gel base, Carbopol was separately dispersed in distilled water and stirred. The solution was allowed to hydrate before adding to the earlier solution. In the last step, the pH of the mixture was adjusted to 6.8 using triethanolamine and subjected to ultrasonic homogenization in order to remove air bubbles and ensure a uniform texture. A similar process was carried out to prepare a blank hydrogel and a hydrogel containing blank niosomes.

Table 3. Composition of the hydrogel

Ingredients	Percentage (%w/w)
Encapsulated AZA/Blank noisome/Free AZA	0.05%
Propylene glycol	1.5%
Glycerin	1.5%
Carbopol 940	0.7%
Methyl paraben	0.2%
Propyl paraben	0.02%
Distilled water	96%
Triethanolamine	until pH is adjusted to 6.8

AZA: azelaic acid

Characterization of niosomal nanocarriers

Physicochemical characterization

After sufficient dilution of aliquots of the niosomal formulations in deionized water at 25 °C, particle size and zeta potentials were investigated (Zetasizer Nano series, Malvern Instruments, ZEN3600, UK. Scanning electron microscopy (SEM) was used for determining morphology and surface properties of blank and AZA-loaded niosomes (MIRA3 TESCAN, Czech Republic). The Fourier Transform Infrared (FT-IR) Spectroscopy analysis of AZA, cholesterol, Span 80, blank niosomes, and AZA-loaded niosomes was conducted using a Bruker instrument (Karlsruhe, Germany).

Encapsulation Efficiency

The synthesized niosomal dispersion was centrifuged (Amicon® Ultra, Millipore) at 10,000 rpm for 20 min at 25 °C. The AZA concentration in the supernatant was determined using a validated spectrophotometric method (Perkin Elmer LAMBDA 15, CA, USA). The entrapment efficiency (EE%) was determined indirectly using the following equation (Eq. 1) [19].

[Downloaded from ajpr.umsha.ac.ir on 2026-11-05]

[DOI: 10.53208/ajpr.6.1.47]

$$EE\% = \frac{\text{Total drug content} - \text{Free drug}}{\text{Total drug content}} \times 100 \quad (1)$$

In vitro release studies

Release of AZA was studied by placing 10 mg of the hydrogels containing AZA niosomes or free AZA in two dialysis bags (MWCO 12,000, Scientific Labs). Dialysis bags were immersed in 250 mL of phosphate-buffered saline (pH 7.4) containing 0.5% (w/v) Span 80, which was stirred at 100 rpm while the temperature was kept at 37 °C using a water bath. At certain intervals, 2 mL of the release medium was taken out and replaced with an equal volume of fresh medium. The AZA concentration was determined using the validated UV spectrophotometric method. This experiment was carried out three times.

Stability studies

Dispersions of AZA-containing niosomes were stored at 25 °C and 4 °C for 3 months in the dark. Samples were collected on days 0, 30, 60, and 90, and analyzed for EE%, particle size, polydispersity index (PDI), and zeta potential.

Characterization of niosomal hydrogels

The pH of the prepared hydrogels was determined after diluting 1 g of the samples in 250 mL of water (4% w/v) using a calibrated pH meter (Sartorius, PB-11) [20]. A rotational viscometer (DVII Digital Viscometer, Brookfield Instruments, UK) with an SC34 spindle was used for investigating rheological properties of the hydrogels.

MTT Assay

The NIH3T3 cell line was used in an MTT (3-(4,5-dimethylthiazol-2-yl)-2,5-diphenyltetrazolium bromide) test to assess the cytotoxicity of the niosomal nanocarriers. The NIH3T3 cells were plated in 96-well plates at a density of 5,000 per well and exposed to different concentrations of free AZA, blank niosomes, and AZA-loaded niosomes for 24 h. There were also control wells that received no treatment. The MTT reagent was added to the wells and incubated for an extra hour to allow the live cells to convert MTT into formazan crystals. Formazan crystals were solubilized in dimethyl sulfoxide, and absorbance was assessed using a microplate reader (Synergy HTX, BioTek Instruments Inc., Winooski, USA).

***In vivo* studies**

Draize Test

The dermal irritation potential of the hydrogels and lactic acid as a positive control was evaluated on healthy female New Zealand White rabbits (3–4 kg, n = 3) in accordance with ISO 10993-10 and approved by the Institutional Ethics Committee of Hamadan University of Medical Sciences. Animals were housed under standard laboratory conditions with free access to food and water. Dorsal fur was clipped 24 h before testing, and the skin was examined to ensure it was intact and free of lesions. Hydrogel specimens were applied to the shaved dorsal skin and secured with a semi-occlusive dressing. After the exposure period, dressings were removed, application sites were gently rinsed with sterile saline, and dermal reactions were scored at 24, 48, and 72 h. Any signs of erythema and edema were assessed using the Draize scale (0–4). Other irritation-related symptoms like dryness, cracking, or blistering were also noted.

Skin Penetration Study

A Franz diffusion cell comprising a recipient chamber with 15.0 mL capacity and 2.54 cm^2 diffusion area, operating at 37 °C, was utilized. A modified technique was used for preparing mouse skin from the abdominal region [21]. Hydrogels containing AZA-loaded noisomes and free AZA were directly applied to the skin, and AZA concentration in the receptor fluid was determined after 2, 4, 6, 8, 12, 16, and 24 h.

Statistical analysis

All experiments were performed in triplicate, and data are presented as Mean ± SD. All charts were drawn using GraphPad Prism (version 7), and the software was used for statistical analysis of data for determination of any significant differences between investigated groups (p<0.05).

[Downloaded from ajpr.umsha.ac.ir on 2026-11-05]

[DOI: 10.53208/ajpr.6.1.47]

Results and Discussion

Experimental design and optimization

Table 4 summarizes the particle size, PDI, and EE% of 15 different AZA-loaded niosomes synthesized according to the Box–Behnken experimental design. Statistical analysis of the obtained data for the highest adjusted and predicted R^2 showed the quadratic linear method as the significant method for predicting particle size and EE%. Table 5 shows the characteristics of the optimized formulation predicted by the significant method.

Table 4. Particle size, PDI, zeta potential, and EE% of the azelaic acid-loaded niosomes prepared according to box–behnken design (n=3)

Run	Particle size (nm)	Zeta potential (mV)	PDI	EE%
1	274.5±16.7	43.16±3.6	0.209±0.048	86.25±5.48
2	265.6±11.3	50.13±5.7	0.321±0.061	84.5±4.35
3	276.8±19.1	54.37±3.1	0.354±0.074	91.42±4.77
4	214.2±13.4	53.24±3.9	0.338±0.085	70.81±5.38
5	482.9±23.4	51.36±2.7	0.549±0. 091	93.43±6.73
6	434.7±27.1	43.73±2.3	0.383±0.070	85.12±9.74
7	216.3±16.2	48.33±3.4	0.445±0.074	75.95±6.17
8	230.8±12.9	55.46±3.1	0.226±0.042	80.23±7.36
9	264.4±18.3	46.83±2.7	0.365±0.083	73.49±6.51
10	287.2±11.5	53.15±3.8	0.417±0.067	96.75±7.72
11	264.7±14.8	46.83±3.2	0.304±0.076	88.56±6.84
12	413.1±18.7	43.17±2.5	0.437±0.039	90.18±8.93
13	184.7±13.6	47.36±2.9	0.293±0.064	67.47±3.65
14	387.4±26.8	45.26±3.6	0.303±0.056	83.73±5.11
15	312.3±15.3	49.83±3.3	0.457±0.080	92.66±8.27

AZA: azelaic acid, PDI: polydispersity index, EE%: entrapment efficiency

Table 5. Results of regression analysis for EE% and particle size

	Model	Adeq Precision	Pred R-square	Adj R-Square	R-Square	SD	%CV	P value
EE%	Quadratic	4.111	0.4363	0.2911	0.7468	7.45	8.92	0.001
Particle size	Linear	5.757	0.0325	0.3611	0.4980	17.54	23.53	<0.0001

EE%: entrapment efficiency

Effect of different formulation variables on the characteristics of the niosomes were shown by polynomial equations (Equations 1,2) and 3D response surface plots (Figure 1). In these plots, A, B, and C indicate AZA amount, total weight of niosomal ingredients, and surfactant: cholesterol ratio.

$$EE\ (\%) = +83.60+10.32 \times A +4.83 \times B +3.64 \times C \quad (1)$$

$$Size=+300.63 +68.69\ A +60.25\ B +19.41C \quad (2)$$

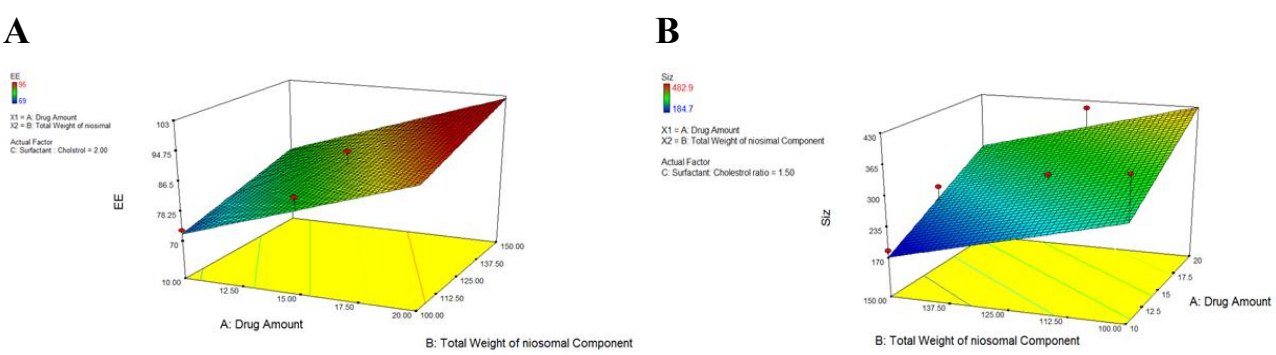


Figure 1. Response plots showing the effect of formulation parameters on A) entrapment efficiency and B) particle size

Niosomes with very small size deliver their content to the deeper layers of the skin [22]. According to Equation 2, both independent variables (drug amount and the total weight of niosomal

[Downloaded from ajpr.umsha.ac.ir on 2026-11-05]

[DOI: 10.53208/ajpr.6.1.47]

components) had a positive effect on the size of niosomes. Primary studies have shown that at a constant total weight of niosome components, increasing the ratio of surfactant to cholesterol from 1 to 2 led to a significant decrease in the size of niosomes. Cholesterol concentration can increase the hydrophobicity of the bilayer, leading to decreased surface free energy and vesicle size [23]. Therefore, further increase of the ratio of surfactant to cholesterol would increase the size of niosomes, probably due to the formation of multilamellar and/or multivesicular particles during the hydration step [25].

The response surface plot for the effect of AZA amount, combined weight of components, and the ratio of surfactant to cholesterol on EE% showed a synergistic influence of all the independent variables on the EE%. A rise in the total fat available for hydration may explain this observation, which results in the formation of multilamellar and/or multivesicular vesicles with greater room for AZA [24].

Finally, in order to reach the optimal conditions, the appropriate ratio of surfactant to cholesterol should be chosen, which will result in having nanoparticles with the right size and the highest possible amount of loading. As mentioned earlier, the size reduction depends on the increase in the surfactant-to-cholesterol ratio, and the right amount of cholesterol is also necessary to achieve the favorable factors mentioned above.

As shown in Table 3, all niosomes had acceptable PDI values of less than 0.5. Zeta potential or total charge of nanovesicles, is commonly used as a diagnostic tool to assess the stability of niosomal dispersions. A colloidal system can be considered stable if its ZP value falls between ±20 mV. The AZA niosomes showed positive zeta potential values, resulting in electrical repulsion between the particles.

Table 6. Suggested formulation by Design Expert® 13.0.0 software

Suggested niosomal formulation			Predicted characteristics		Observed characteristics	
Drug amount (mg)	Niosome amount (mg)	cholesterol: surfactant (v/v)	Particle size (nm)	EE (%)	Particle size (nm) Mean±SD	EE (%) Mean±SD
20	150	1.54	274.359	95.123	287.2±2.12	96.1±1.3

EE%: entrapment efficiency

Characterization of the niosomes

Figure 2 displays SEM image of the optimized formulation of AZA-loaded niosomes. It can be observed that niosomes are formed as spherical particles with a uniform shape and size.

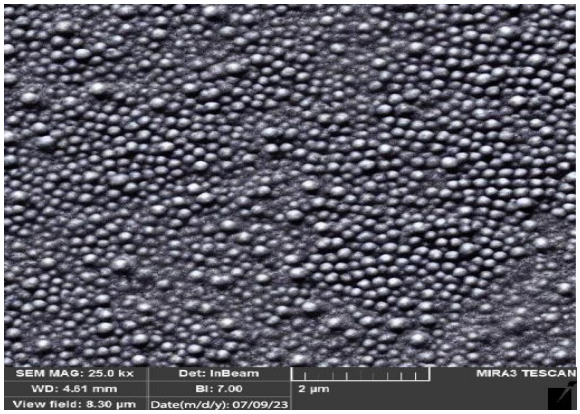


Figure 2. Scanning electron microscopy image of the optimized formulation of azelaic acid-loaded niosomes

Figure 3 shows FT-IR spectra of blank and AZA-loaded niosomes along with the ingredients used for preparing them. The FT-IR spectrum of Span 80 shows distinct absorptions at (1173,1085), (2925,2855), and 3399 cm^{-1} related to C–O, C–H, and O–H stretching, respectively. For cholesterol, noticeable absorptions were detected at 2,800–3,000, 3452, 1,035–1,378, 1,506, and 1,674 cm^{-1} corresponding to C–H, O–H, CH_2 bending, C–C in aromatic ring, and C=C.

Blank niosomes showed absorptions at 1,125 and 1,747 cm^{-1}, indicating the presence of a combination of Span 80 and cholesterol. The FT-IR spectrum of AZA shows typical bands coming from the aliphatic chain at 2,926 cm^{-1} and 2,840 cm^{-1} as well as a high intensity band related to two free carboxyl groups at 1,688 cm^{-1}. The FT-IR spectrum of AZA-loaded niosomes shows successful encapsulation of AZA in niosomal nanocarriers. For example, the C=O stretching peak of AZA at 1,688 cm^{-1} is observed

[Downloaded from ajpr.umsha.ac.ir on 2026-11-05]

[DOI: 10.53208/ajpr.6.1.47]

with some shift to 1693 cm^{-1} and reduced intensity, and CH_2 stretching peaks at 2,840 cm^{-1} and 2,926 cm^{-1} have shifted to 2,845 cm^{-1} and 2,932 cm^{-1} [28, 29].

Stability of azelaic acid-loaded niosomes

Results of the stability tests, including particle size, PDI, zeta potential, and EE% are presented in Table 7. As can be deduced from these data, the optimized formulation demonstrated excellent stability in terms of particle size, polydispersity index, zeta potential, and encapsulation efficiency while displaying no evidence of aggregation, precipitation, or phase separation throughout a 90-day storage period at both 25 °C and 4 °C. It can be concluded that this niosomal formulation stays stable for at least three months when stored at 4 °C or room temperature.

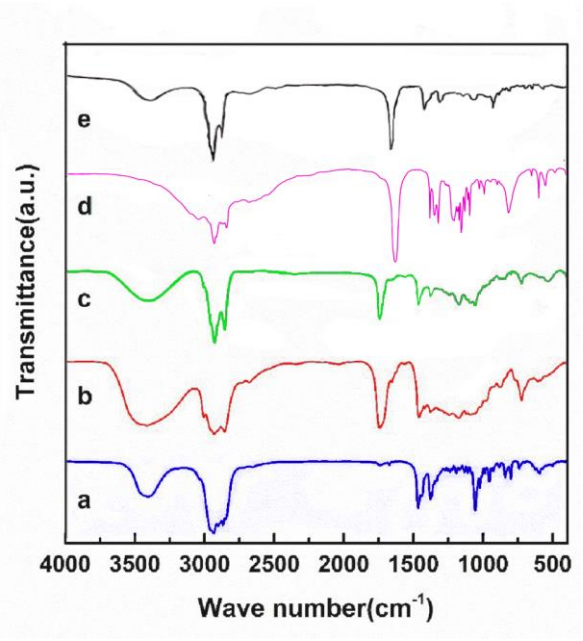


Figure 3. Fourier Transform Infrared spectra of a) Cholesterol, b) Span 80, c) blank niosomes, d) azelaic acid, and e) azelaic acid-loaded niosomes

Table 7. Size, PDI, zeta potential, and EE% of stability samples of the optimized azelaic acid-loaded niosomes. Results are shown as mean ± SD (n=3)

Temperature	Day of storage	Size (nm)	PDI	Zeta potential (mV)	EE (%)
4 ºC	0	287.12±8.5	0.6±0.038	53.5±2.1	96.37±4.32
	30	311.37±9.2	0.5±0.042	49.8±3.4	94.29±3.8
	60	301.48±7.1	0.5±0.028	55.1±2.7	93.41±4.79
	90	324.59±9.7	0.5±0.034	61.9±2.9	91.58±3.83
25 ºC	0	281.82±6.8	0.6±0.047	51.3±3.2	91.75±4.21
	30	308.36±7.3	0.5±0.033	48.5±2.2	89.52±3.48
	60	319.18±8.9	0.5±0.021	52.7±3.5	87.19±4.06
	90	362.04±9.4	0.5±0.039	63.1±3.1	87.94±3.88

AZA: azelaic acid, PDI: polydispersity index, EE%: entrapment efficiency

Characterization of the hydrogels

Figure 4 shows digital images of four hydrogel formulations, including blank hydrogel, and hydrogels containing free AZA, blank niosomes, and AZA-loaded niosomes. All hydrogels demonstrated a consistent and uniform texture, with a milky white appearance and were devoid of any observable particles. Physical characteristic of the hydrogels containing free AZA or AZA-loaded niosomes are summarized in Table 8. Both pH and viscosity did not show significant difference in the two investigated hydrogels. Moreover, obtained values are appropriate for topical preparations [27].

Table 8. Physical properties of the hydrogels. Results are shown as mean ± SD (n=3)

Formulation	pH	Homogeneity	Viscosity (cP)	Appearance
AZA niosomal hydrogel	7.3±0.4	good	14500±842	Milky white
Free AZA hydrogel	6.95±0.2	good	13810±630	Transparent, colorless

AZA: azelaic acid

[Downloaded from ajpr.umsha.ac.ir on 2026-11-05]

[DOI: 10.53208/ajpr.6.1.47]

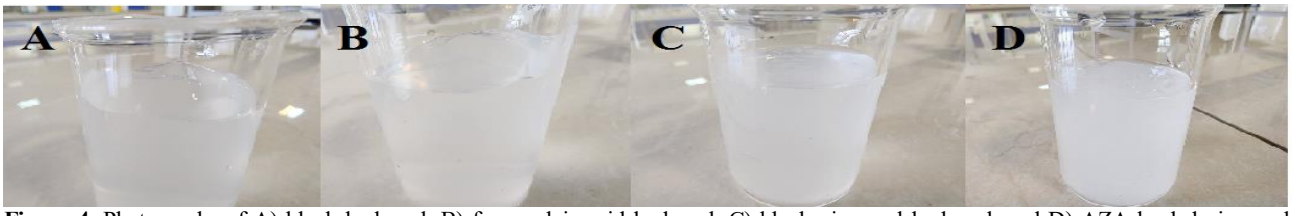


Figure 4. Photographs of A) blank hydrogel, B) free azelaic acid hydrogel, C) blank niosomal hydrogel, and D) AZA-loaded niosomal hydrogel

In Vitro release studies

Release profile of the hydrogels containing free AZA (HD) or AZA-loaded niosomes (HND) are shown in Figure 5. Niosomal hydrogel showed nearly complete release of AZA during 24 h. It also showed a prolonged release profile with slower release rate after the first 8 h. On the other hand, free AZA hydrogel showed a rapid release profile, with 45.3% ± 1.89 of the total AZA released within the first hour compared with 11.3% ± 0.92 for the niosomal hydrogel.

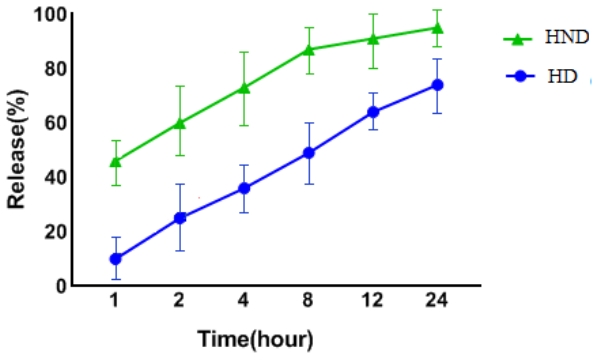


Figure 5. Release profile of azelaic acid from the prepared hydrogels (n=3, error bars show SD)

The two primary mechanisms that limit the rate of drug release from nanocarriers are the rate of diffusion and dissolution [30]. The lipophilic nature of AZA is the reason for its slow release after being entrapped in lipid matrix of the niosomes [31].

Skin permeability test

Figure 6 shows profile of permeation of AZA from the hydrogels containing free AZA (HD) or AZA-loaded niosomes (HND). Results showed greater capacity of the niosomal hydrogel for delivering AZA to the skin in comparison to the hydrogel containing free AZA. Both profiles showed a significant decrease in the rate of AZA permeation through the skin after the first 8 h. Moreover, the niosomal hydrogel was found to significantly enhance drug concentration in the epidermis and dermis layers, compared to the free AZA hydrogel (p<0.05). Cumulative amounts of permeated AZA were 77.9 ± 4.9 µg/cm^2 and 93.4 ± 6.1 µg/cm^2 for free and niosomal hydrogels, respectively.

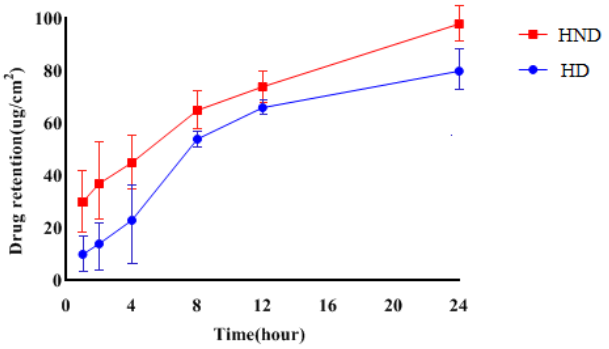


Figure 6. Percentage of azelaic acid passed through mouse skin after 24 h (n=3, error bars show SD).

MTT test

Figure 7 shows outcomes of MTT assays investigating the impact of hydrogels containing free AZA (HD) or niosomal AZA (HND), along with blank niosomes (HN) on cells viability. It was found that the viability of NIH3T3 cell line increased upon increasing the free AZA concentration over 48 h, demonstrating a dose-dependent proliferative effect. A previous study has reported the anti-proliferative activity of AZA on mouse keratinocytes which is in line with its beneficial effect in some skin disorders caused by alteration of keratinocytes differentiation [32].

However, the amount of AZA loaded in the hydrogel or niosomes in the present study is much lower than the concentration range tested in this study. These results indicate that AZA can be a proliferative agent at low concentrations. The hydrogel containing blank niosomes showed toxic effect at concentrations higher that 5 µg/ml. Previous studies have shown the same dose-dependent toxicity for blank niosomes that helps the

[Downloaded from ajpr.umsha.ac.ir on 2026-11-05]

[DOI: 10.53208/ajpr.6.1.47]

researchers determine the safe concentration of the niosomal material in the formulation. The same dose-dependent toxicity was observed for the hydrogel containing AZA loaded niosomes. However, due to the protective effect of AZA, significant toxicity was observed at 10 µg/ml, compared with the control. Overall, it can be concluded that the AZA-loaded niosomal preparation should be used at safe concentrations within the hydrogel formulation.

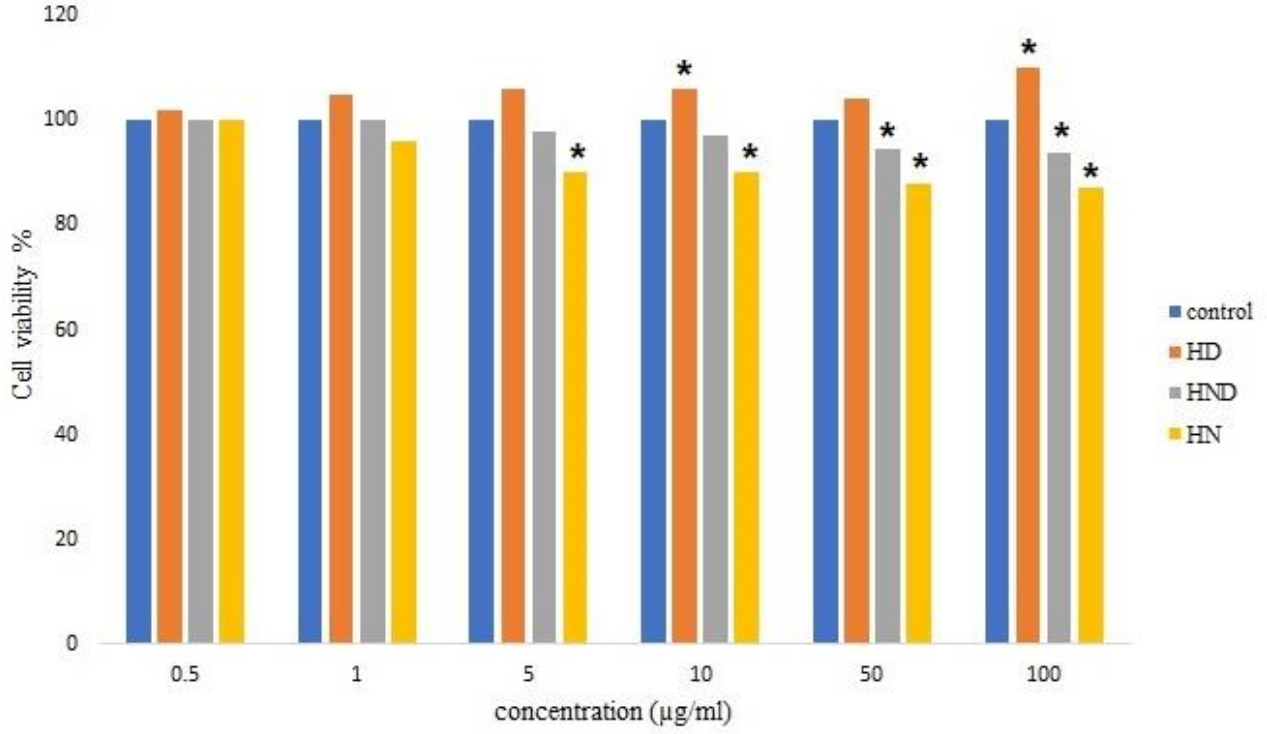


Figure 7. Percent viability of NIH3T3 cells treated with different concentrations of samples (n=3, error bars show SD)

Draize test

Based on the results of the Draize test (Table 9), application of AZA-loaded niosomal hydrogel did not cause any skin irritation. No signs of erythema or edema was observed in the treated skin areas throughout the 3-day treatment period as shown in Figure 8. Furthermore, absence of dryness, cracking, or blistering indicates the non-irritant nature of the formulation. Therefore, these nanocarriers can be deemed appropriate for topical drug delivery in the treatment of androgenic alopecia, given their minimal propensity to cause skin irritation or any unfavorable reactions [33].

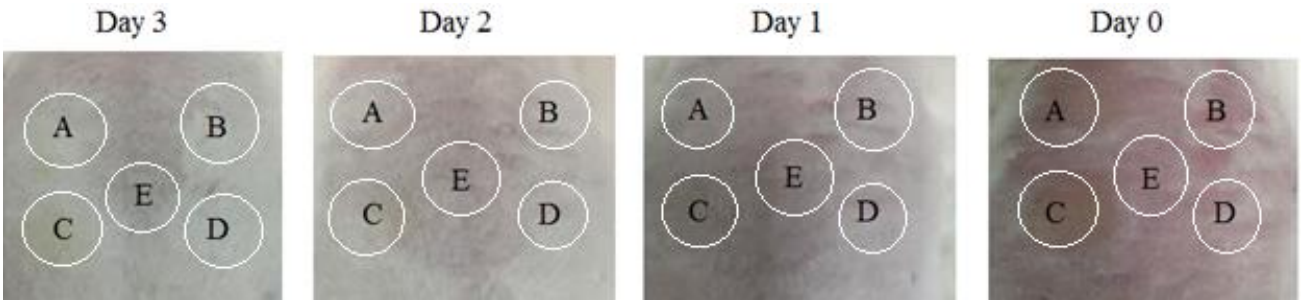


Figure 8. Photographs of rabbit skin after 72 h of treatment with A) free AZA hydrogel, B) blank niosomal hydrogel, C) azelaic acid niosomal hydrogel, D) blank hydrogel, and E) control

[Downloaded from ajpr.umsha.ac.ir on 2026-11-05]

[DOI: 10.53208/ajpr.6.1.47]

Table 9. Mean erythemal scores observed for skin application of the prepared hydrogels after 24, 48, and 72 h

	Groups									
	Control +		Blank hydrogel		Free AZA hydrogel		AZA niosomal hydrogel		Blank niosomal hydrogel	
	Erythema	Edema	Erythema	Edema	Erythema	Edema	Erythema	Edema	Erythema	Edema
24	2	0	0	0	0	0	0	0	0	0
48	1	0	0	0	0	0	0	0	0	0
72	1	0	0	0	0	0	0	0	0	0

Conclusion

Results of this study suggest that AZA in nano-niosomes particles is a promising candidate for the development of topical formulations for the treatment of skin disorders and hair loss. The physicochemical properties of AZA in nano-niosomes particles ensure its stability and efficient delivery to the target site. Furthermore, its ability to inhibit 5-alpha reductase enzyme activity and promote hair growth makes it a potential therapeutic agent for androgenic alopecia.

However, further studies are needed to address several important aspects. First, it is essential to evaluate the pharmacokinetic and pharmacodynamic profiles of the niosomal nanocarriers in human subjects to confirm their safety and efficacy. Second, it is necessary to optimize the formulation of the niosomal nanocarriers to improve their stability and drug entrapment efficiency. Third, it is important to investigate the effect of the niosomal nanocarriers on other aspects of hair growth, such as hair thickness and density. Finally, it is crucial to determine the potential side effects of the niosomal nanocarriers, such as skin irritation or allergic reactions, in a large population of subjects.

Credit authorship contribution statement

OmidKeshvariSharif: Investigation, Formal analysis, Writing – original draft**.**

Shabnam pour moslemi and Seyed Yaser Vafaei: Resources, Writing – review & editing, Supervision, and Funding.

Rasool Haddadi: Advisers, Writing – review & editing.

Declaration of Competing Interest

The authors declare that they have no conflict of interest.

Acknowledgments

This research was the Pharm. D thesis of the first author that was supported by the Vice Chancellor for Research and Technology in Hamadan University of Medical Sciences.

References

1. Stevens J, Khetarpal S. Platelet-rich plasma for androgenetic alopecia: a review of the literature and proposed treatment protocol. Int J Womens Dermatol. 2019;5(1):46-51. [DOI: 10.1016/j.ijwd.2018.08.004] [PMID] [PMCID]
2. English RS Jr. A hypothetical pathogenesis model for androgenic alopecia: clarifying the dihydrotestosterone paradox and rate-limiting recovery factors. Med Hypotheses. 2018;111:73-81. [DOI: 10.1016/j.mehy.2017.12.027] [PMID]
3. Georgescu SR, Amuzescu A, Mitran CI, Mitran MI, Matei C, Constantin C, et al. Effectiveness of platelet-rich plasma therapy in androgenic alopecia-a meta-analysis. J Pers Med. 2022;12(3):342. [DOI: 10.3390/jpm12030342] [PMID] [PMCID]
4. Singh SK, Chaubey S, Bansal A, Kaur G, Malik DS. Cosmeceutical aptitudes of azelaic acid. Curr Drug Res Rev. 2021;13(3):222-229. [DOI: 10.2174/2589977513666210526122909] [PMID]
5. Spaggiari C, Annunziato G, Spadini C, Montanaro SL, Iannarelli M, Cabassi CS, et al. Extraction and quantification of azelaic acid from different wheat samples (Triticum durum Desf.) and evaluation of their antimicrobial and antioxidant activities. Molecules. 2023;28(5):2134. [DOI: 10.3390/molecules28052134] [PMID] [PMCID]
6. Draelos ZD, Elewski B, Staedtler G, Havlickova B. Azelaic acid foam 15% in the treatment of papulopustular rosacea: a randomized, double-blind, vehicle-controlled study. Cutis. 2013;92(6):306-317. [PMID]
7. Amirfakhryan E, Davarnia B, Jeddi F, Najafzadeh N. Azelaic acid stimulates catalase activation and promotes hair growth through upregulation of Gli1 and Gli2 mRNA and Shh protein. Avicenna J Phytomed. 2020;10(5):460-471. [PMID] [PMCID]
8. Yang K, Tang Y, Ma Y, Liu Q, Huang Y, Zhang Y, et al. Hair growth promoting effects of 650 nm red light stimulation on human hair follicles and study of its mechanisms via RNA sequencing transcriptome analysis. Ann Dermatol. 2021;33(6):553-561. [DOI: 10.5021/ad.2021.33.6.553] [PMID] [PMCID]

[Downloaded from ajpr.umsha.ac.ir on 2026-11-05]

[DOI: 10.53208/ajpr.6.1.47]

9. Espinosa Arriaga M, Palacios Rodriguez AP, García-Contreras R, Hu Oxte GE, Sanchez Magaña M, Martinez Gonzalez G, Ramirez Villalva A, Almeida J. Azelaic Acid as a Novel Antivirulence Agent Against Pseudomonas aeruginosa: In silico, In vitro and In vivo Efficacy and Biocompatibility. vitro and In vivo Efficacy and Biocompatibility. 10.64898/2026.03.18.712801] [PMID] [PMCID]
10. Pan Y, Liu D, Wei Y, Su D, Lu C, Hu Y, et al. Azelaic acid exerts antileukemic activity in acute myeloid leukemia. Front Pharmacol. 2017;8:359. [DOI: 10.3389/fphar.2017.00359] [PMID] [PMCID]
11. Burger C, Shahzad Y, Brummer A, Gerber M, du Plessis J. Traversing the skin barrier with nano-emulsions. Curr Drug Deliv. 2017;14(4):458-472. [DOI: 10.2174/1567201813666160824125444] [PMID]
12. Mota AH, Rijo P, Molpeceres J, Reis CP. Broad overview of engineering of functional nanosystems for skin delivery. Int J Pharm. 2017;532(2):710-728. [DOI: 10.1016/j.ijpharm.2017.07.078] [PMID]
13. Mullick P, Hegde AR, Gopalan D, Pandey A, Nandakumar K, Jain S, et al. Evolving era of "sponges": nanosponges as a versatile nanocarrier for the effective skin delivery of drugs. Curr Pharm Des. 2022;28(23):1885-1896. [DOI: 10.2174/1381612828666220518090431] [PMID]
14. Sankar R, Jain SK. Development and characterization of gastroretentive sustained-release formulation by combination of swelling and mucoadhesive approach: a mechanistic study. Drug Des Devel Ther. 2013;7:1455-1469. [DOI: 10.2147/DDDT.S52890] [PMID] [PMCID]
15. Lopes VF, Giongo CN, de Almeida Campos L, Abraham WR, Mainardes RM, Khalil NM. Chitosan nanoparticles potentiate the in vitro and in vivo effects of curcumin and other natural compounds. Curr Med Chem. 2021;28(24):4935-4953. [DOI: 10.2174/0929867328666201124152945] [PMID]
16. Momekova DB, Gugleva VE, Petrov PD. Nanoarchitectonics of multifunctional niosomes for advanced drug delivery. ACS Omega. 2021;6(49):33265-33273. [DOI: 10.1021/acsomega.1c05083] [PMID] [PMCID]
17. Asthana GS, Sharma PK, Asthana A. In vitro and in vivo evaluation of niosomal formulation for controlled delivery of clarithromycin. Scientifica (Cairo). 2016;2016:6492953. [DOI: 10.1155/2016/6492953] [PMID] [PMCID]
18. Pardakhty A, Varshosaz J, Rouholamini A. In vitro study of polyoxyethylene alkyl ether niosomes for delivery of insulin. Int J Pharm. 2007;328(2):130-141. [DOI: 10.1016/j.ijpharm.2006.08.002] [PMCID]
19. Ourique AF, Pohlmann AR, Guterres SS, Beck RCR. Tretinoin-loaded nanocapsules: preparation, physicochemical characterization, and photostability study. Int J Pharm. 2008;352(1-2):1-4. [DOI: 10.1016/j.ijpharm.2007.12.035] [PMID]
20. Mandawgade SD, Patravale VB. Development of SLNs from natural lipids: application to topical delivery of tretinoin. Int J Pharm. 2008;363(1-2):132-138. [DOI: 10.1016/j.ijpharm.2008.06.028] [PMID]
21. Abdallah MH, Abu Lila AS, Unissa R, Elsewedy HS, Elghamry HA, Soliman MS. Brucine-loaded ethosomal gel: design, optimization, and anti-inflammatory activity. AAPS PharmSciTech. 2021;22(8):269. [DOI: 10.1208/s12249-021-02113-8] [PMID]
22. Chinembiri TN, Gerber M, du Plessis LH, du Preez JL, Hamman JH, du Plessis J. Topical delivery of Withania somnifera crude extracts in niosomes and solid lipid nanoparticles. Pharmacogn Mag. 2017;13(Suppl 3):S663-S671. [DOI: 10.4103/pm.pm_489_16] [PMID] [PMCID]
23. Ghosh S, Roy A, Banik D, Kundu N, Kuchlyan J, Dhir A, et al. How does the surface charge of ionic surfactant and cholesterol forming vesicles control rotational and translational motion of rhodamine 6G perchlorate (R6G ClO4)? Langmuir. 2015;31(8):2310-2320. [DOI: 10.1021/la504819v] [PMID]
24. Waqas MK, Sadia H, Khan MI, Omer MO, Siddique MI, Qamar S, et al. Development and characterization of niosomal gel of fusidic acid: in-vitro and ex-vivo approaches. Des Monomers Polym. 2022;25(1):165-174. [DOI: 10.1080/15685551.2022.2086411] [PMID] [PMCID]
25. Moghddam SRM, Ahad A, Aqil M, Imam SS, Sultana Y. Formulation and optimization of niosomes for topical diacerein delivery using 3-factor, 3-level Box-Behnken design for the management of psoriasis. Mater Sci Eng C Mater Biol Appl. 2016;69:789-797. [DOI: 10.1016/j.msec.2016.07.043] [PMID]
26. Ullah S, Khalid R, Rehman MF, Irfan MI, Abbas A, Alhoshani A, et al. Biosynthesis of phyto-functionalized silver nanoparticles using olive fruit extract and evaluation of their antibacterial and antioxidant properties. Front Chem. 2023;11:1202252. [DOI: 10.3389/fchem.2023.1202252] [PMID] [PMCID]
27. Hong SK, Eastham JA, Fine SW. Localization of higher grade tumor foci in potential candidates for active surveillance who opt for radical prostatectomy. Prostate Int. 2013;1(4):152-157. [DOI: 10.12954/PI.13029] [PMID] [PMCID]
28. Hsieh PW, Al-Suwayeh SA, Fang CL, Lin CF, Chen CC, Fang JY. The co-drug of conjugated hydroquinone and azelaic acid to enhance topical skin targeting and decrease penetration through the skin. Eur J Pharm Biopharm. 2012;81(2):369-378. [DOI: 10.1016/j.ejpb.2012.03.006] [PMID]
29. Kumar A, Rao R, Yadav P. Azelaic acid: a promising agent for dermatological applications. Curr Drug Ther. 2020;15(3):181-193. [DOI: 10.2174/1574885514666190904160228]
30. Hamed R, Al Baraghthi T, Sunoqrot S. Correlation between the viscoelastic properties of the gel layer of swollen HPMC matrix tablets and their in vitro drug

[Downloaded from ajpr.umsha.ac.ir on 2026-11-05]

[DOI: 10.53208/ajpr.6.1.47]

release. Pharm Dev Technol. 2018;23(9):838-848. [DOI: 10.1080/10837450.2016.1257022] [PMID]
31. Alminger M, Aura AM, Bohn T, Dufour C, El SN, Gomes A, et al. In vitro models for studying secondary plant metabolite digestion and bioaccessibility. Compr Rev Food Sci Food Saf. 2014;13(4):413-436. [DOI: 10.1111/1541-4337.12081] [PMID]
32. Detmar M, Mayer-da-Silva A, Stadler R, Orfanos CE. Effects of azelaic acid on proliferation and ultrastructure of mouse keratinocytes in vitro. J Invest Dermatol. 1989;93(1):70-74. [DOI: 10.1111/1523-1747.ep12277353] [PMID]
33. Lee HJ, Oh DW, Na MJ, Kim DW, Yuk DY, Choi HC, et al. Preparation and in vivo evaluation of lecithin-based microparticles for topical delivery of minoxidil. Arch Pharm Res. 2017;40(8):943-951. [DOI: 10.1007/s12272-017-0934-x] [PMID]

[Downloaded from ajpr.umsha.ac.ir on 2026-11-05]

[DOI: 10.53208/ajpr.6.1.47]